ASME 2008 Dynamic Systems and Control Conference
October 20-22, 2008, Ann Arbor, Michigan, USA

DSCC2008

LONGITUDINAL VEHICLE DYNAMICS SCALING AND IMPLEMENTATION ON A HIL SETUP

Rajeev Verma*
Systems Laboratory
University of Michigan
Ann Arbor, Michigan 48109
Email: rajverma@umich.edu

Domitilla Del Vecchio
Systems Laboratory
University of Michigan
Ann Arbor, Michigan 48109
Email: ddv@eecs.umich.edu

Hosam K. Fathy
Department of Mechianical Engineering
University of Michigan
Ann Arbor, Michigan 48109
Email: hfathy@umich.edu

ABSTRACT

This paper presents the application of Buckingham's π theorem to scale the powertrain of a High Mobility Multipurpose Wheeled Vehicle (HMMWV) by deriving non dimensional ratios called π parameters. A Hardware In the Loop (HIL) setup is constructed and the resulting longitudinal dynamics of the scaled vehicle are validated against those of a full scale vehicle model. This is performed with the ultimate goal of testing cooperative collision avoidance algorithms on a testbed comprising a number of these scaled vehicles.

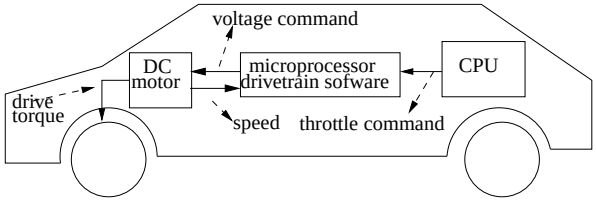

Figure 1: HIL setup. The hardware of the vehicle includes chassis, wheels, axis, and a DC motor with encoder. The scaled drivetrain dynamics is implemented on the microprocessor controlling the DC motor.

1 INTRODUCTION

In this paper, we consider the problem of scaling the drivetrain dynamics of a High Mobility Multipurpose Wheeled Vehicle (HMMWV) and the problem of implementing the scaled dynamics in a hardware-in-the-loop (HIL) setup. This is performed with the ultimate goal of developing a scaled experimental testbed. This testbed will be used to validate decision and control algorithms for intelligent transportation systems (ITS) applications.

ITS include cooperative intersection collision avoidance systems, lateral collision avoidance systems, and longitudinal collision avoidance systems [3,14]. Testing autonomous or partly autonomous algorithms directly on a full scale transportation system is difficult due to cost limitations and safety constraints. We are thus developing a lab-scale testbed composed of 1/13 scale vehicles to validate decision and control algorithms for cooperative intersection collision avoidance systems. In such a testbed, the vehicles are equipped with wireless communication, with a positioning system emulating GPS, and with on-board computers solving decision, control, and communication tasks. The vehicle's longitudinal dynamics play a central role in collision avoidance algorithms. For a meaningful algorithm validation, it is therefore crucial to design scaled vehicles whose dynamics faithfully reproduce the longitudinal dynamics of a full scale vehicle. We do not address the lateral vehicle dynamics in this paper.

Our scaled vehicle hardware is composed only of the chassis including wheels, tires, driveshaft, and a DC motor with encoder. The unavailability of exact scaled replicas of the engine and transmission makes it difficult to include a physical drivetrain on the prototype. Therefore, a HIL setup is designed in which a microprocessor controlling the DC motor emulates the scaled drivetrain dynamics of a HMMWV including its engine and transmission. This HIL setup takes as input a throttle command and applies to the wheels the desired drive torque. This way, we obtain a scaled vehicle that as a whole responds to throttle commands in a way similar to the full scale vehicle (Figure 1). In this paper, we focus on the development and validation of this HIL setup. In particular, the scaling of the drivetrain dynamics, including active components such as the engine, is performed by applying well-known concepts from scaling theory, including the Buckingham π theorem.

*Address all correspondence to this author.

A historical account of the development of similitude theory can be found in [5,6,19]. Researchers have been studying scaled vehicles since 1930s in the context of trailer sway [9], vehicle dynamics [1,21], performance on rough terrain and determining vehicle turning radius [1], and automobile accident reconstruction [10]. More recently, work has been reported in areas of vehicle dynamics and controls [4–6,8], study of the lateral vehicle motion and design of steering controllers [7,15], control prototyping for Anti-lock Braking System (ABS) [17,18], and investigation of vehicle rollover [20]. The work in the literature has focused mostly on lateral dynamics. The unique contribution of this paper is the demonstration of longitudinal dynamics scaling of a vehicle with all the active powertrain subsystems present in it using a HIL approach. Our validation experiments confirm that the longitudinal response of the scaled vehicle matches the longitudinal response of a full scale vehicle model.

This paper is organized as follows. Next section lists all the symbols used in the paper. In Section 2, we describe the drivetrain model that we consider. In Section 3, we perform the computation of the π groups and simulate the scaled model to show the match with the full scale model. In Section 4, we implement the scaled dynamics on the microprocessor. In Section 5, we show experimental results and validate the obtained data against the simulation data of the scaled model.

NOMENCLATURE

ρ_{air} Air density (Kg/m^3).
g Acceleration due to gravity (m/s^2).
θ_{CS} Angular displacement of flywheel ($radian$).
θ_i Angular displacement of turbine ($radian$).
θ_t Angular displacement of transmission ($radian$).
θ_p Angular displacement of propeller shaft ($radian$).
ρ Average density of vehicle material (Kg/m^3).
τ_{brake} Brake torque (Nm).
B Damping coefficient of transmission ($\frac{Kgm^2}{radian\ s}$).
R_{dcm} DC motor armature resistance (ohm).
K_τ DC motor torque coefficient (Nm/amp).
K_B DC motor back EMF coefficient ($volts/radian$).
I DC motor current ($ampere$).
L_{dcm} DC motor armature inductance ($henry$).
θ DC motor angular displacement ($radian$).
C_D Drag coefficient ([ ]).
τ_w Drive shaft output torque (Nm).
J_e Flywheel moment of inertia (Kgm^2).
i_t Gear ratio ([ ]).
τ_i Impeller torque (Nm).
U Longitudinal speed of the vehicle (m/s).
τ_d Output torque produced by final drive (Nm).
θ_f Output angular displacement of final drive ($radian$).
θ_w Output angular displacement of drive shaft ($radian$).
A_f Projected front area of the vehicle (m^2).
τ_p Propeller shaft input torque (Nm).
τ_f Propeller shaft output torque (Nm).
V_{PWM} PWM voltage signal applied to DC motor ($volt$).
C_{rr} Rolling resistance coefficient ([ ]).
θ_{road} Road gradient ($radian$).
K Stiffness of transmission ($Nm/radian$).
R Tire radius (m).
K_{fc} Torque converter capacity factor ($\frac{radian}{Kg^{0.5}m}$).
T_{ratio} Torque converter torque ratio ([ ]).
N_{ratio} Torque converter speed ratio ([ ]).
τ_t Torque output of the torque converter (Nm).
τ_m Torque produced by DC motor (Nm).
τ_e Torque produced by the engine (Nm).
I_t Transmission inertia (Kgm^2).
τ_t Turbine torque (Nm).
m Vehicle mass (Kg).
l Vehicle track length (m).
J_w Wheel inertia (Kgm^2).

2 Drivetrain model

The nonlinear differential algebraic equations corresponding to each component of the drivetrain and of the vehicle are described in [11–13,16]. Here, such components are briefly described. Figure 2 shows the schematic of a vehicle drivetrain. We consider a 4 speed vehicle with automatic transmission and rear wheel drive.

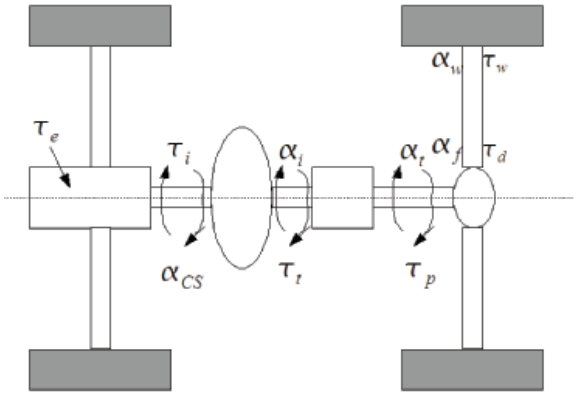

Figure 2: DRIVETRAIN.

The engine produces torque resulting from the combustion process. The engine is modeled as a map (Figure 3), which takes throttle command and engine speed as input and calculates torque generated by the engine, τ_e. For the low frequency dynamics we are interested in, a map based engine model can be used. The engine's flywheel is modeled as an inertia. The governing equation for the engine and the flywheel is $J_e\ddot{\theta}_{CS} = \tau_e - \tau_i$, where J_e is the engine and flywheel moment of inertia, $\ddot{\theta}_{CS}$ is the acceleration of the flywheel, τ_e is the torque produced by the engine and τ_i is the impeller torque. Engine acceleration is calculated from this equation, which takes as input engine torque, τ_e, and load torque from the torque converter, τ_i.

The torque converter model is a tabular relationship between the impeller torque, τ_i, the turbine torque, τ_t, the impeller speed,

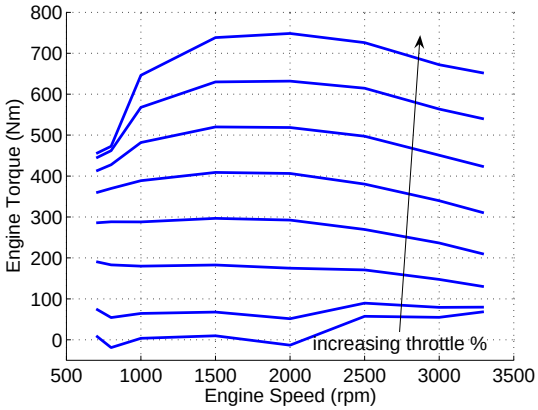

Figure 3: ENGINE MAP [11].

which is assumed to be equal to $\dot{\theta}_{CS}$, and the turbine speed, $\dot{\theta}_i$. The inputs to this model are speed ratio, $N_{ratio} = \frac{\dot{\theta}_i}{\dot{\theta}_{CS}}$, and impeller speed. The capacity factor, K_{fc}, and the torque ratio, T_{ratio}, can be determined from a map (refer to [11]). The impeller torque and turbine torque are calculated from the equations $\tau_i = \frac{\dot{\theta}_{CS}^2}{K_{fc}{}^2}$ and $\tau_t = T_{ratio}\tau_i$.

The transmission is modeled as a variable gear ratio transformer. To derive transmission dynamics, we treat it as a mass-spring-damper system with damping coefficient B, inertia I_t, and stiffness K. This system takes as input the torque output of the torque converter, τ_t, and the gear ratio, i_t. It produces propeller shaft input torque, τ_p. Refer to [16] for more details.

Gear shifting is modeled using a shift map (refer to [11]), which takes propeller shaft speed and throttle position commanded by the driver as the input and determines the instantaneous gear ratio as the output. Torque and speed variations during the gear shift are captured by incorporating a blending function into the model. The blending function (refer to [11]) gives the variation of torque ratio and speed ratio during the gearshift and captures important dynamics observed during a gearshift [11, 16].

The propeller shaft input torque, τ_p, and speed, $\dot{\theta}_t$, are equal to the output torque, τ_f, and speed, $\dot{\theta}_p$.

The final drive is modeled as a ratio, i_f, which reduces the input speed, $\dot{\theta}_p$, and increases the input torque, τ_f, to produce the output speed, $\dot{\theta}_f$, and torque, τ_d, respectively. This is modeled by $\tau_d = \tau_f i_f$ and $\theta_p = \theta_f i_f$. The drive shaft input torque, τ_d, and speed, $\dot{\theta}_f$, are equal to the output torque, τ_w, and speed, $\dot{\theta}_w$.

A point mass vehicle model is considered here as we consider only longitudinal vehicle dynamics. The longitudinal motion of the vehicle is defined by:

$$(J_w + mR^2)\ddot{\theta}_w = \tau_w - \tau_{brake} - \frac{\rho_{air}}{2} C_D A_f U^2 R - C_{rr} mgR - Rmgsin(\theta_{road}), \quad (1)$$

where J_w is the wheel inertia, m is the mass of the vehicle, τ_{brake} is the brake torque, U is the longitudinal vehicle velocity, ρ_{air} is the air density, C_D is the drag coefficient, A_f is the projected front area of the vehicle, C_{rr} is the rolling resistance coefficient, R is the tire radius, and θ_{road} is the road gradient, assumed 0 here.

The system described above constitutes a point mass longitudinal dynamics model that does not account for roll and pitch. The model considered serves well the purpose of predicting the behavior of a HMMWV in longitudinal maneuvers and is simple enough to be programmable on the motion controller, given its processing and memory constraints.

3 Scaling

To apply Buckingham's π theorem to the system described in Section 2 the governing dynamical equations are examined. Parameters and variables associated with the system that are used in this study are listed in Table 1.

Table 1: PARAMETERS ASSOCIATED WITH THE VEHICLE IN TERMS OF FUNDAMENTAL QUANTITIES.

Parameter	Fundamental quantity
N_{ratio}, T_{ratio}, i_t, i_f	$[M^0L^0T^0]$
θ_{CS}, θ_i, θ_t, θ_p, θ_f, θ_w	$[M^0L^0T^0]$
$Throttle, Brake$	$[M^0L^0T^0]$
τ_e, τ_i, τ_t, τ_p, τ_f, τ_d, τ_w, τ_{brake}	$[M^1L^2T^{-2}]$
J_e, I_t, J_w	$[M^1L^2T^0]$
m	$[M^1L^0T^0]$
R, l	$[M^0L^1T^0]$
U	$[M^1L^0T^{-1}]$
ρ, ρ_{air}	$[M^1L^{-3}T^0]$
K_{fc}	$[M^{-0.5}L^{-1}T^0]$
A_f	$[M^0L^2T^0]$
B	$[M^1L^2T^{-2}]$
C_D, C_{rr}	$[M^0L^0T^0]$

The fundamental quantities (basic units) chosen for the formulation of nondimensional groups (π groups) are M, T, L. Similitude is achieved by grouping the parameters into $(n-m)$ independent nondimensional groups, where n is the number of parameters and m is the number of fundamental quantities.

All of the dimensionless parameters, such as angles and percentages, form their own π groups. We have 3 fundamental dimensions and 34 parameters (Table 1). Out of these, if we choose m, U and l as repeating parameters (parameters that can appear in

some or all of the π groups), the remaining parameters will form 31 dimensionless π groups.

Table 2: π GROUPS ASSOCIATED WITH THE SYSTEM.

π Groups	Interpretation
$\pi_1 = Throttle, \pi_2 = Brake$	Non-dimensional driver inputs
$\pi_3 = i_t$, $\pi_4 = i_f$, $\pi_5 = N_{ratio}$, $\pi_6 = T_{ratio}$	Non-dimensional transmission and final drive gear ratio
$\pi_7 = \frac{J_e}{mL^2}$, $\pi_8 = \frac{I_t}{mL^2}$, $\pi_9 = \frac{J_w}{mL^2}$	Non-dimensional engine, transmission and wheel inertia
$\pi_{10} = \theta_{CS}$, $\pi_{11} = \theta_i$, $\pi_{12} = \theta_t$, $\pi_{13} = \theta_p$,$\pi_{14} = \theta_f$, $\pi_{15} = \theta_w$	Non-dimensional angular displacements
$\pi_{16} = \frac{\tau_e}{mU^2}$, $\pi_{17} = \frac{\tau_i}{mU^2}$, $\pi_{18} = \frac{\tau_t}{mU^2}$, $\pi_{19} = \frac{\tau_p}{mU^2}$, $\pi_{20} = \frac{\tau_f}{mU^2}$, $\pi_{21} = \frac{\tau_d}{mU^2}$, $\pi_{22} = \frac{\tau_w}{mU^2}$, $\pi_{23} = \frac{\tau_{brake}}{mU^2}$	Non-dimensional torques
$\pi_{24} = K_{fc}\sqrt{mL^2}$	Non-dimensional capacity factor
$\pi_{25} = \frac{R}{l}$	Non-dimensional wheel radius
$\pi_{26} = \frac{\rho L^3}{m}$, $\pi_{27} = \frac{\rho_{air} L^3}{m}$	Non-dimensional vehicle and air density
$\pi_{28} = \frac{A_f}{l^2}$	Non-dimensional projected front area of vehicle
$\pi_{29} = \frac{B}{mUL}$	Non-dimensional damping
$\pi_{30} = C_D$, $\pi_{31} = C_{rr}$	Non-dimensional drag and rolling resistance coefficient

A list of all the π groups is given in Table 2.

3.1 Design of the scaled vehicle

It follows from Buckingham π theorem that if two dynamical systems are described by the same differential equations, then the solution to these differential equations will be scale-invariant if the π groups are the same. To design the scaled vehicle, we thus start with analyzing the π groups given in Table 2. For the scaled vehicle to be dynamically similar to the full scale vehicle, the value of these π groups should be the same for both systems. Based on this concept, we can match the parameters of the scaled vehicle to those of the full scale vehicle.

3.1.1 Calculation of parameter values for the scaled vehicle The track length of the full scale vehicle and of the scaled vehicle are fixed. The tire size of the scaled vehicle is calculated by equating the π group corresponding to the tire size of the scaled vehicle to the π group of the full scale vehicle (Table 2-row 8), that is, $\left(\frac{R}{l}\right)_{full} = \left(\frac{R}{l}\right)_{Scaled}$. Substituting the value of $R_{full} = 0.4412$, $l_{full} = 3.302$ and $l_{Scaled} = 0.257$, we obtain $R_{scaled} = 0.0343m$. From the available tire prototypes, a tire of radius $0.033\ m$ is selected for the scaled vehicle prototype.

The mass of the scaled vehicle is 3.15 Kg. To calculate the mass of the full scale vehicle, we equate the π groups corresponding to the vehicle density (Table 2-row 9). We obtain, $\left(\frac{\rho l^3}{m}\right)_{Scaled} = \left(\frac{\rho l^3}{m}\right)_{full}$. It is assumed that $(\rho)_{Scaled} = (\rho)_{full}$. Substituting $m_{Scaled} = 3.15$, $l_{full} = 3.302$ and $l_{Scaled} = 0.257$, m_{full} can be calculated to be $6681Kg$.

Note that the gross vehicle weight of the full scale vehicle is 5112 Kg [11]. In this paper it is assumed that the full scale vehicle is carrying a payload of 1569 Kg. The vehicle model that is used in this work is of an upgraded, joint light tactical vehicle HMMWV that can carry such a high payload.

To find the ratio of velocity that the scaled vehicle should maintain with respect to the full scale vehicle in response to the same input, first observe that time is not being scaled. Thus, we can consider Ut/l to form another π group. Equating this π group for the scaled and full scale vehicle, we have $\left(\frac{Ut}{l}\right)_{Scaled} = \left(\frac{Ut}{l}\right)_{full}$, which gives the relation $\frac{U_{full}}{U_{Scale}} = 3.302/0.257 = 12.84$. Thus, the full scale vehicle velocity should be 12.84 times the velocity of the scaled vehicle when the same maneuver is performed on both systems.

The moment of inertia of the engine in the full scale HMMWV, J_e, is $0.5\ Kg\,m^2$ [12]. To calculate the moment of inertia of the engine in the scaled vehicle, we equate the corresponding π terms to obtain $\left(\frac{J_e}{ml^2}\right)_{Scaled} = \left(\frac{J_e}{ml^2}\right)_{full}$. Substituting the parameter values and solving for $J_{eScaled}$, we obtain $J_{eScaled} = 1.51 * 10^{-6}$.

To determine the ratio of torque produced by the engine of the scaled vehicle to the full scale vehicle, the π groups corresponding to engine torque are equated (Table 2-row 6), that is, $\left(\frac{\tau_e}{mU^2}\right)_{Scaled} = \left(\frac{\tau_e}{mU^2}\right)_{full}$. Substituting the parameter values gives the relation between $(\tau_e)_{Scaled}$ and $(\tau_e)_{full}$ as $(\tau_e)_{Scaled} = 2.855 * 10^{-6}(\tau_e)_{full}$. This torque scaling is used to scale the engine torque map (Figure 3).

It is difficult to measure parameters such as $I_t, J_w, A_f, B, C_D, C_{rr}$ for the scaled vehicle. The difference in these parameters is compensated as described in Section 4.2.

3.2 Validation of the scaled model

The validation of the derived π groups and scaled vehicle design based on these groups is performed in two steps. A simulation of the scaled model is carried out as a first step. This is followed by experimental tests with the scaled vehicle hardware. These are discussed in Section 5.

Parameters of the scaled model are derived as illustrated in Section 3.1. The full scale and scaled vehicle simulation are

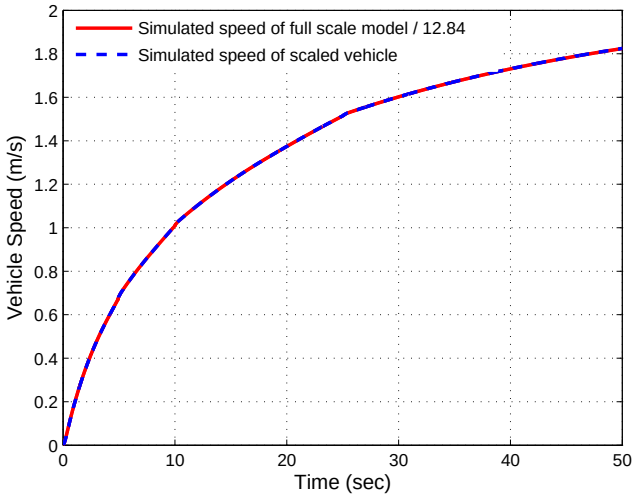

Figure 4: SCALED VEHICLE VELOCITY VERSUS FULL SCALE VEHICLE VELOCITY.

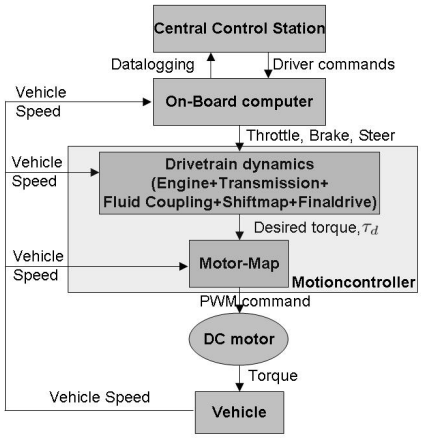

Figure 5: SCALED VEHICLE COMMAND FLOW.

carried out for the same input commands. It is found that the longitudinal velocity of the full scale vehicle is 12.84 times the velocity of the scaled vehicle, as shown in the Figure 4.

4 Implementation on the scaled vehicle

A scaled radio controlled (RC) car chassis [1] is used as the hardware platform to implement the scaled dynamics and validate the simulation results.

Figure 5 shows the system architecture. In the present configuration, a human driver issues throttle commands through a central control station. These commands are transmitted to the on-board computer through a wireless connection. These commands act as an input to the driveline dynamics which are programmed on the motion controller. The next section describes the hardware and software setup of the scaled vehicle.

4.1 Description of the scaled vehicle setup

In this section, specifications of the scaled vehicle are provided. The scaled vehicle wheelbase is 257mm. The scaled vehicle uses a replaceable brush standard type electric motor.

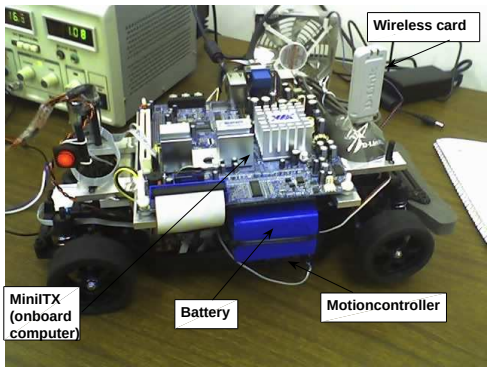

Figure 6: SCALED VEHICLE.

Each vehicle (Figure 6) is equipped with a motion controller (BrainStem Module) implementing the scaled driveline dynamics of a HMMWV (Section 2). The drivetrain components, including engine, fluid coupling, transmission, gear shift logic and final drive are programmed on the motion controller. The shift logic is programmed in the form of a shift map. The output of this program is the drive torque, τ_d. The motion controller issues control signals to the steering servo and controls the PWM (pulse width modulation) signal to the DC motor through a 3 Amp H-Bridge. The programming on the motion controller is performed in the Tiny Embedded Application (TEA) [2] language, which is a subset of the C programming language.Vehicle speed is measured using an optical encoder and is used for calculations in the drivetrain and motor map blocks.The front axle of the vehicle is modified to fit the encoder and it no longer drives the vehicle. Thus, the vehicle has rear wheel drive and front wheel steering.

The on board computer (running Linux, Fedora core) communicates with the motion controller by means of a serial connection. It is equipped with wireless communication capability. It handles the high level control functions by commanding steering, braking and throttle to the motion controller. A datalogging module is programmed on the on board computer, which can read vehicle speed from the motion controller at a frequency of 10 samples/s. This speed is transmitted to a central control station through a wireless connection, where it is recorded.

The drive torque, τ_d, is the torque that should be applied to the wheels. Since we have a DC motor, it is difficult to measure

[1] http://www.tamiyausa.com/

[2] www.acroname.com/brainstem/TEA/tea1.html

or control such a torque because of the absence of current measurement. To overcome this problem, a set of experiments were performed to identify the relationship between drive torque and motor voltage for any given wheel speed. This is discussed in the next section.

4.2 DC motor system identification

The dynamics of the electromechanical system comprising a car being run by the DC motor includes three parts: (1) A dynamic mechanical subsystem, which is the scaled vehicle, (2) a dynamic electrical subsystem, which includes all of the motor's electrical effects, and (3) a static relationship which represents the conversion of electrical quantities into mechanical torque. Assuming very high torsional stiffness of the drivetrain components transmitting torque, the mechanical subsystem dynamics of the vehicle run by a permanent magnet brush DC motor are assumed to be of the form

$$M\ddot{\theta} + B_v\dot{\theta} = \tau_m, \tag{2}$$

in which $M = J_w + mR^2$ and $\tau_m = K_\tau I$. Here J_w is the wheel inertia, m is the scaled vehicle mass, R is the wheel radius of the scaled vehicle, B_v is the coefficient of viscous friction in the drivetrain, τ_m is the torque produced by the DC motor, θ is the angular motor position, K_τ is the coefficient which characterizes the electromechanical conversion of armature current to torque, and I is the motor armature current. The current, I, is given by the electrical subsystem dynamics for the permanent magnet brush DC motor, which is assumed to be of the form:

$$L_{dcm}\dot{I} = V_{PWM} - R_{dcm}I - K_B\dot{\theta}, \tag{3}$$

in which L_{dcm} is the armature inductance, R_{dcm} is the armature resistance, K_B is the back-emf coefficient (which is equal to K_τ), and V_{PWM} is the Pulse Width Modulation voltage signal supplied to the DC motor. For the above model, the states θ and $\dot{\theta}$ are easy to measure while I is difficult to measure. Because of the inability to measure the motor current I, the control of the torque produced by the motor is hard. This difficulty is overcome by noticing that in this mechatronic systems, the time constant of the electrical subsystem is faster than the mechanical subsystem (L_{dcm} in equation (3) is very small). This means that we can assume the current and voltage to be statically related. Assuming L_{dcm} to be negligible, we can write equation (3) as:

$$I = \frac{V_{PWM}}{R_{dcm}} - \frac{K_B\dot{\theta}}{R_{dcm}}. \tag{4}$$

From equation (2), we have, substituting $\tau_m = K_\tau I$,

$$M\ddot{\theta} + \left(B_v + K_\tau\frac{K_B}{R_{dcm}}\right)\dot{\theta} - K_\tau\frac{V_{PWM}}{R_{dcm}} = 0, \tag{5}$$

in which $M\ddot{\theta}$ is the torque that accelerates the vehicle. We call it the total torque i.e., $\tau_{total} := M\ddot{\theta}$. It is equal to the torque produced by the motor minus the torque lost in damping of the scaled vehicle. Our objective is to control the torque generated by the DC motor, τ_m, and make it equal at all time to the torque generated by the engine, τ_e, that is programmed on the motion controller. As stated earlier, this is a hard problem in the absence of current measurement. In order to solve this problem, we identify the coefficients of $\dot{\theta}$ and of V_{PWM} in equation (5) by running experiments.We have that τ_d is the torque that is calculated by the HIL simulation of the drivetrain and it accelerates the vehicle while, τ_{total} is the torque that corresponds to the actual acceleration of the vehicle. Thus, we shift the problem from trying to make τ_e equal to τ_m to making τ_{total} equal to τ_d. This is feasible because τ_{total} can be determined experimentally.

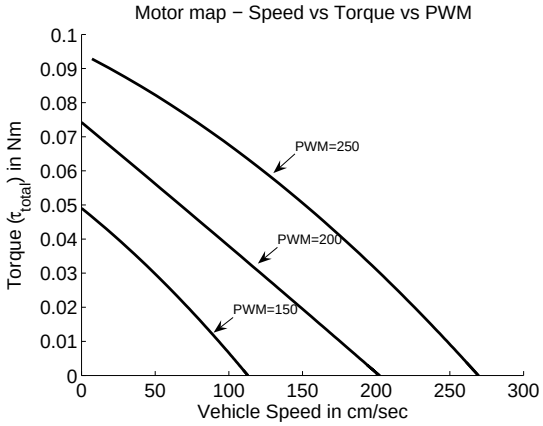

Figure 7: MOTOR MAP.

Experiments performed involve applying a constant PWM signal (V_{PWM}) to the DC motor and recording the vehicle response (vehicle velocity versus time). The data is logged at a frequency of 7.7 Hz. Vehicle acceleration is obtained by differentiating vehicle velocity. As vehicle velocity is noisy, a polynomial fit of the third order to the vehicle velocity versus time curve is used before differentiation to calculate the acceleration a. The value of $\ddot{\theta}$ is calculated from this acceleration as follows:

$$\ddot{\theta}_w = \frac{a}{R} \tag{6}$$

$$\ddot{\theta} = 7.21\ddot{\theta}_w, \tag{7}$$

where $\ddot{\theta}_w$ is the wheel angular acceleration and 7.21 is the gear ratio of the scaled model.

A number of such experiments are performed, for a particular PWM, to check the repeatability of the experiment. PWM signals are chosen to cover the whole range of operation of the DC motor. Rewrite equation (5) as:

$$V_{PWM} = k_1\tau_{total} + k_2 v, \tag{8}$$

where v is the vehicle velocity, k_1 and k_2 are constants. Based on these experiments, the values of k_1 and k_2 are found to be 250 and 1, respectively.

A motor map is obtained by plotting τ_{total} versus vehicle velocity at a constant PWM value as shown in Figure 7. To use this map on a running vehicle at any instant of time, the drivetrain block (Figure 5) calculates the torque (τ_d) that is to be applied to the scaled vehicle. The PWM that has to be supplied to the DC motor to generate this torque, given the velocity of the scaled vehicle τ_d can be calculated from equation (8) (by replacing τ_{total} by τ_d).

Experiments are conducted to verify the longitudinal response of the scaled vehicle versus the response predicted by the simulation. In these experiments, a constant throttle input of 30 %, 40 % and 50 % is applied to the vehicle and the simulated and experimental vehicle response are compared. However, as discussed in Section 3.1, parameters such as I_t, J_w, A_f, B, C_D and C_{rr} are difficult to measure. Thus, the response of the scaled vehicle is expected to be different from that of the simulation. To compensate for this, the parameters in equation (8) are further tuned to obtain a good match between the observed and simulated response. The tuned parameter values obtained for 30%, 40% and 50% throttle are not significantly different. Thus, the final form of equation (8) is $V_{PWM} = 70 + 2800\tau_d + 0.72v$, in which the parameters obtained in correspondance to 30 % throttle are used.

5 Experiments

A number of experiments were performed to ascertain the behavior of the scaled vehicle and its dynamic similitude to a HMMWV. The following sections discuss the experimental setup and results.

5.1 Experimental Setup

The scaled vehicle takes throttle commands from the human driver at a central control station. The driving maneuver that is considered for verifying the longitudinal response of the scaled vehicle *vis-a-vis* a full scale vehicle is a constant throttle performance test. In this test, a constant throttle input is given to the scaled vehicle and the resulting velocity and gear shift response are logged. This test is repeated for several throttle values $(30\%, 40\%, 50\%)$. These tests are performed in a 43 meter long corridor, which is covered by the wireless network.

A constant voltage of 15.4 volts is employed to power the scaled vehicle during the tests. Since the purpose of this testbed is to test algorithms for cooperative collision avoidance at traffic intersections and because of the size of the testbed, we do not expect to attain neither high velocity nor the steady state velocity of the vehicle. Therefore the throttle is limited to a value of up to 50% and only the transient speed response is validated.

It is observed during the experiments that the scaled vehicle does not start as soon as the throttle command is applied by the driver. This can be attributed to adhesion between moving parts in the scaled vehicle hardware where solid-solid contact occurs. This phenomenon is widely studied and a good review is provided in [2]. This issue is not addressed in the present work and is left for future consideration. We have thus adopted an ad-hoc approach of applying enough initial torque to the stationary vehicle to make it overcome the initial adhesion.

5.2 Experimental Results

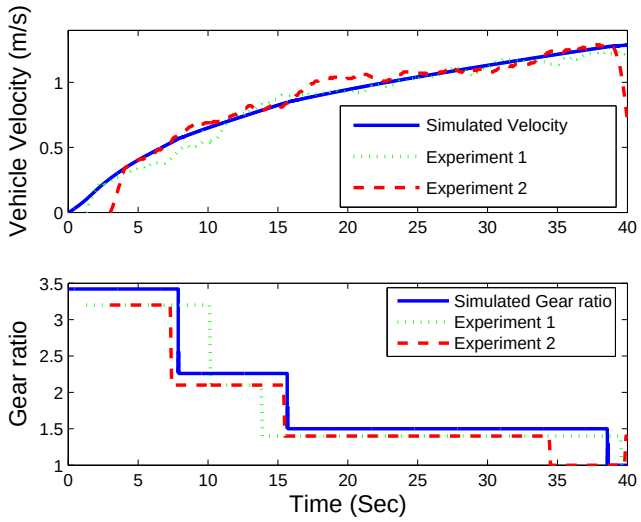

Figure 8: VEHICLE SPEED AND GEAR RATIO VERSUS TIME FOR SCALED VEHICLE MODEL AND SCALED VEHICLE SIMULATION.

The results are presented for a constant input of 30 %, 40 % and 50 % throttle. Figure 8 shows the speed response of the scaled vehicle *vis-a-vis* simulation. It is seen that the response of the scaled vehicle closely follows the simulated response. The average root mean square (RMS) error in speed for 30 % throttle is 0.0525m/s, for 40 % throttle is 0.0809m/s and for 50 % throttle is 0.1099m/s. There seems to be an increasing trend in the RMS error. This, in part, can be attributed to the higher speeds attained by the vehicle with increasing throttle because of which we normalize the RMS error with maximum speed. The normalized RMS error attained by the vehicle with 30 %, 40 % and 50 % is 0.4375, 0.559 and 0.605, respectively. The lower error for the 30 % throttle can be attributed to the fact that the motor map parameters were chosen so as to obtain the best results for the 30 % throttle (as explained in Section 4.2).

Figure 8 shows the time instants at which gear shifts take place for the scaled vehicle and the simulated vehicle. It is seen that the errors in gear shifting events at 30 % throttle are 1.25 *sec* for 1st to 2nd gearshift, 1 *sec* for 2nd to 3rd gearshift, and 2.5 *sec* for 3rd to 4th gearshift. For 40 % throttle, the errors are 1 *sec* for 1st to 2nd gearshift, 1.8 *sec* for 2nd to 3rd gearshift, and 3.3 *sec* for 3rd to 4th gearshift. For 50 % throttle the errors are 0.45 *sec* for 1st to 2nd gearshift, 1.6 *sec* for 2nd to 3rd gearshift, and 4.5 *sec* for 3rd to 4th gearshift. These errors can be explained as follows. Transmission gear shift timing is governed by shift maps,

which dictate the vehicle's gear ratio as a function of driver throttle position and propeller shaft speed. The output of such shift map, namely, the gear ratio, is often quite sensitive to small variations in velocity. This sensitivity of gear shift to vehicle and engine speed is well-recognized in the literature and is often exacerbated in real vehicles by the fact that driver throttle position is itself often a function of vehicle speed. A significant literature studies such gear hunting [3] and develops control techniques for mitigating it. In this work, we consider errors in gear shift timing acceptable if they do not result in significant errors in vehicle velocity. Since gear shift has a direct impact on transmission output torque, which in turn affects vehicle velocity through an integration operator, we expect errors in gear shift timing to undergo some attenuation as they propagate into vehicle velocity errors. Experimental results in Figure 8 confirm this and show that while errors in gear shift timing are significant, commensurate errors in vehicle velocity are much smaller. Thus, we consider the scaled vehicle presented herein successfully validated.

6 Conclusions

The development of a scaled vehicle that is dynamically similar to a HMMWV is presented. Models of various subsystems of the full scale vehicle are introduced and the scaled vehicle design is carried out. Implementation on a scaled RC car is performed. Experiments demonstrate the dynamic similitude of the scaled vehicle to the full scale vehicle.

ACKNOWLEDGMENT

This work was supported by NSF CAREER award number CNS-0642719.

REFERENCES

[1] M. G. Bekker. *Introduction to TerrainVehicle Systems*. The University of Michigan Press, Ann Arbor, 1959.

[2] B. Bhushan. Adhesion and stiction: Mechanisms, measurement techniques, and methods for reduction. *Journal of vacuum science and technology*, 21(6):2262–2296, Nov-Dec 2003.

[3] R. Bishop. *Intelligent Vehicle Technology And Trends*. Artech House, Inc., Norwood, MA, 2005.

[4] S. Brennan and A. Alleyne. The Illinois roadway simulator: A mechatronic testbed for vehicle dynamics and control. *IEEE/ASME Trans. on Mech. Sys.*, 5(4):349–359, 2000.

[5] S. N. Brennan. Modeling and control issues associated with scaled vehicles. Master's thesis, University of Illinois at Urbana Champaign, 1999.

[6] S. N. Brennan. *On size and control: the use of dimensional analysis in controller design*. PhD thesis, University of Illinois at Urbana Champaign, 2002.

[7] S. R. Burns, Jr. R. T. O'Brien, and J. A. Piepmeier. Steering controller design using scale-model vehicles. *Proceedings of the Thirty-Fourth Southeastern Symposium on System Theory*, pages 476–478, 2002.

[8] M. DePoorter, S. Brennan, and A. Alleyne. Driver assisted control strategies: Theory and experiment. In *Proc. ASME Int. Mech. Eng. Congr. Expo.*, pages 721–728, 1998.

[9] L. Huberand O. Dietz. Pendelbewegungen von lastkraftwagenanhangern und iner vereidung (snaking of truck trailers). *VDI-zeit schrift*, 81(16):459–463, 1937.

[10] R. I. Emori. Automobile accident reconstruction. Technical report, UCLA Motor Vehicle Safety Contract Final Report, UCLA Schools of Engineering and Medicine, 1969.

[11] H. Fathy, R. Ahlawat, and J. L. Stein. Proper powertrain modeling for engine-in-the-loop-simulation. In *Proceedings of the ASME International Engineering Congress and Exposition, number IMECE2005-81592, 2006*, volume 74, pages 1195–1201, New York.

[12] Z. Filipi, H. Fathy, J. R. Hagena, A. Knafl, R. Ahlawat, J. Liu are D. Jung, D. N. Assanis, H. Peng, and J. Stein. Engine-in-the-loop testing for evaluating hybrid propulsion concepts and transient emissions - HMMWV case study. In *SAE 2006 World Congress and Exhibition, Detroit, MI, USA*, 2006.

[13] T. D. Gillespie. *Fundamentals of Vehicle Dynamics*. SAE International, March 1992.

[14] Intelligent Vehicle Initiative. Final report. *Available at http://www.itsdocs.fhwa.dot.gov/JPODOCS/REPTS_PR/14153_files/ivi.pdf*, 2005.

[15] R.T. O'Brien Jr., J.A. Piepmeier, P.C. Hoblet, S.R. Burns, and C.E. George. Scale-model vehicle analysis using an off-the-shelf scale-model testing apparatus. In *American Control Conference*, pages 3387–3392, 2004.

[16] U. Kiencke and L. Nielsen. *Automotive Control Systems, For Engine, Driveline, and Vehicle*. Springer Verlag, 2nd edition, 2005.

[17] R. G. Longoria, A. Al-Sharif, and C. Patil. Scaled vehicle system dynamics and control: A case study on anti-lock braking. *International Journal of Vehicle Autonomous Systems*, 2(1-2):18–39, 2004.

[18] A. Mathews. Implementation of a fuzzy rule based algorithm for adaptive antilock braking in a scaled car. Master's thesis, University of Texas at Austin, 2002.

[19] M. Polley, A. Alleyne, and E. De Vries. Scaled vehicle tire characteristics: dimensionless analysis. *Vehicle Systems Dynamics*, 44(2):87–105, February 2006.

[20] R. J. Whitehead, D. M. Bevly, and B. Clark. Esc effectiveness during property variations on scaled vehicles. In *ASME IMECE*, pages 233–242, November 2005.

[21] Ya. H. Zakin. Pritchine vozniknovenya pritsepov (the cause of instability of trailers). *Avtom. Promyshlennost (Russian Automotive Industry Journal)*, 11, 1959.

[3] Shift hunting prevention for an automatic transmission, Patent number 5669850, Sept 1997